

The X-ray Asynchronous Optical Afterglow of GRB 060912A and Tentative Evidence of a 2175-Å Host Dust Extinction Feature

J. Deng¹, W. Zheng^{1,*}, M. Zhai¹, L. Xin¹, Y. Qiu¹, A. Stefanescu^{2,**}, A. Pozanenko³,
M. Ibrahimov⁴, A. Volnova⁵

ABSTRACT

We present optical photometry of the GRB 060912A afterglow obtained with ground-based telescopes, from about 100 sec after the GRB trigger till about 0.3 day later, supplemented with the *Swift* optical afterglow data released in its official website. The optical light curve (LC) displays a smooth single power-law decay throughout the observed epochs, with a power-law index of about -1 and no significant color evolution. This is in contrast to the X-ray LC which has a plateau phase between two normal power-law decays of a respective index of about -1 and -1.2. It is shown by our combined X-ray and optical data analysis that this asynchronous behavior is difficult to be reconciled with the standard afterglow theory and energy injection hypothesis. We also construct an optical-to-X-ray spectral energy distribution at about 700 sec after the GRB trigger. It displays a significant flux depression in the *B*-band, reminding us of the possibility of a host-galaxy (at $z = 0.937$) 2175-Å dust absorption similar to the one that characterizes the Milky Way extinction law. Such an identification, although being tentative, may be confirmed by our detailed analysis using both template extinction laws and the afterglow theory. So far the feature is reported in very few GRB afterglows. Most seem to have a host galaxy either unusually bright for a GRB, just like this one, or of an early type, supporting the general suggestion of an anti-correlation between the feature and star-forming activities.

¹National Astronomical Observatories, 20A Datun Road, Chaoyang District, Beijing 100012, China; jsdeng@bao.ac.cn

²Max-Planck-Institut für Extraterrestrische Physik, Giessenbachstrabe, 85740 Garching, Germany

³Space Research Institute of RAS, Profsoyuznaya, 84/32, Moscow 117997, Russia

⁴Ulugh Beg Astronomical Institute, Tashkent 700052, Uzbekistan

⁵Sternberg Astronomical Institute, Moscow State University, Moscow 119992, Russia

*now at Department of Physics, University of Michigan, Ann Arbor, MI 48109, USA

**now at Max-Planck-Institut Halbleiterlabor, Otto-Hahn-Ring 6, 81739 München, Germany and Johannes Gutenberg-Universität, Inst. f. anorganische und analytische Chemie, 55099 Mainz, Germany

1. Introduction

The launch of *Swift* satellite in late 2004 has brought about a new era in the field of gamma-ray bursts (GRBs). More than 95% of the ~ 100 *Swift* GRBs reported each year had their afterglows detected in X-rays and about 60% detected in the optical, which in turn led to a large fraction of *Swift* GRBs having redshift determination and detailed studies (Gehrels, Ramirez-ruiiz & Fox 2009). New questions have also arisen as the cases of well-observed afterglows keep accumulating, which pose new challenges to the standard GRB afterglow model (for recent reviews see Zhang 2007a,b; Granot 2008; Panaitescu 2008b; Gehrels, Ramirez-ruiiz & Fox 2009). One of these puzzles is the occasional lack of an optical light curve (LC) behavior synchronous to a LC break of the X-ray afterglow that usually indicates the end of a shallow decay phase (e.g., Fan & Piran 2006; Panaitescu et al. 2006; Melandri et al. 2008; but see Oates et al. 2009).

The incredible brightness of GRBs makes them excellent probes of the distant universe, e.g., to explore the dust extinction properties of their host environments. Typical attempts involve fitting the afterglow spectral energy distributions (SEDs) with template extinction laws, although a more sophisticated approach based on a parameterized model has been proposed (Li et al. 2008). Most studies favor a Small Magellanic Cloud (SMC) extinction law (Stratta et al. 2004; Kann, Klose & Zeh 2006; Starling et al. 2007; Schady et al. 2007). However, the broad 2175-Å bump characteristic of the Milky Way (MW) extinction law (also marginally appearing in that of the Large Magellanic Cloud (LMC)), whose physical carrier remains a long-standing mystery (Drain 2003), was recently identified in a small number of GRBs (Krühler et al. 2008; Elíasdóttir et al. 2009; Prochaska et al. 2009; Liang & Li 2009).

In this paper, we present the observations of the *Swift* GRB 060912A optical afterglow, which shows a LC behavior inconsistent with that of the X-ray one, and possible evidence of a 2175-Å host dust extinction feature in the SED. The gamma-ray and X-ray properties of the GRB are summarized in §2. Our ground-based observations and the telescopes used, as well as the *Swift* Ultra-Violet and Optical Telescope (UVOT) data that are extracted from the official online catalogue, are described in §3. Combined analysis of the optical and X-ray data are detailed in §4, within the context of the standard afterglow model and energy injection hypothesis while also revealing discrepancies to the models. An optical-to-X-ray SED is built in §5, and the presence of the 2175-Å feature is argued for through extinction template fitting after an simplified correction for H Lyman absorption. A discussion on the implications of our results is given in §6.

2. Gamma-Ray and X-Ray Characteristics

GRB 060912A triggered the *Swift* Burst Alert Telescope (BAT) and Konus-Wind (Hurkett 2006a; Golenetskii et al. 2006). Its single-pulse LC lasted for a duration of $T_{90} \sim 6 - 8$ sec, and hence a long burst as confirmed by spectral lag analysis (Parsons et al. 2006) and by its star-forming host galaxy at $z = 0.937$ (Levan et al. 2007). The BAT data were fitted with a power-law spectrum of a photon index $\Gamma_{\text{BAT}} \approx -1.74$ and a fluence of $\sim 1.35 \times 10^{-6}$ erg cm^{-2} (Sakamoto et al. 2008). The rest-frame E_{peak} may be ~ 150 keV according to Liang, Zhang & Zhang (2007) (based on an empirical $E_{\text{peak}}^{\text{obs}} - \Gamma_{\text{BAT}}$ correlation; see also Sakamoto et al. 2009). Assuming a high-energy index of between -2 and -3 , the isotropic luminosity is $\sim 0.7 - 1 \times 10^{52}$ erg, satisfying the Amati relationship within 2σ (e.g., Amati et al. 2008)

Liang, Zhang & Zhang (2007) re-analyzed the X-ray afterglow data of the GRB as observed with the *Swift* X-Ray Telescope (XRT), independent of the preliminary results of Hurkett, Page & Rol (2006b). For the time-integrated XRT spectrum ($[0.3 - 10 \text{ keV}]$), they obtained a photon index of $\Gamma_{\text{X}}^{\text{mid}} = -2.08 \pm 0.11$ before $\sim 1,350$ sec and of $\Gamma_{\text{X}}^{\text{late}} = -1.95 \pm 0.13$ after that, correcting for absorption by both the Galaxy and the host galaxy. The fitting H-column density assuming a solar metallicity was $N_{\text{H}}^{\text{host}} \approx 4.2 \times 10^{21} \text{ cm}^{-2}$ at $z = 0.937$ for the host galaxy and about $3.8 \times 10^{20} \text{ cm}^{-2}$ for the Galactic value in the GRB direction.

We reproduce in Figure 1 (*open circles*) the XRT LC as reduced by those authors, which consists of an early deep decay before ~ 350 sec, a late deep decay after $\sim 1,800$ sec, and a plateau in between. The three LC segments can be fitted using power law $f_{\text{X}} \propto t^{\alpha}$ separately, with the power-law indices being $\alpha_{\text{X}}^{\text{early}} = -1.04 \pm 0.16$, $\alpha_{\text{X}}^{\text{mid}} = -0.19 \pm 0.08$, and $\alpha_{\text{X}}^{\text{late}} = -1.19 \pm 0.05$, which is consistent with the smoothed broken power-law model results in that paper.

3. Optical Afterglow Observations

3.1. Xinglong Observations

The 0.8-m Tsinghua-NAOC Telescope (TNT) at the Xinglong Observatory automatically observed the GRB upon receiving the GCN alert. The telescope is equipped with standard Johnson-Cousin *UBVRI* filters and a Princeton Instrument 1340×1300 CCD, resulting a field of view of $\sim 11' \times 11'$. For the details of the Xinglong GRB follow-up system, see Zheng et al. (2008) and Deng et al. (2006, 2008).

The TNT observation started ~ 24 sec earlier than the UVOT and lasted for more than

3.7 hr. It began with a preset sequence of unfiltered exposures, i.e., in a *white* band, and was later switched to the filtered bands. Extra observations were made with a 60-cm telescope. The afterglow was detected in the *white* and *R* bands, but not in the *B* and *V* bands.

The observation results are tabulated in Table 1. The data were reduced using IRAF in a standard routine, bias subtracted and flat-fielded. Differential PSF photometry was performed using 8 reference stars, which were calibrated in a photometric night. Since the response curve of our CCD peaks in the *R* band, we used the *R*-band magnitudes of the reference stars for the *white* band and assumed that the so-derived afterglow magnitudes are equivalent to *R*-band ones. Our independent photometric tests with stellar objects have shown this to be a decent assumption, introducing a typical scatter of only ~ 0.07 mag.

3.2. Maidanak Observations

The 1.5-m telescope of Maidanak Observatory is located at the south-east of Uzbekistan. Its follow-up observations were made in both the *R* and *B* bands from about 3 to 6 hours after the GRB onset under favorable weather and seeing of $\sim 0.6''$, using an SITe 2000×800 CCD with a field of view of $\sim 8.5' \times 3.5'$. The data were reduced in the same way as the Xinglong data, using the same set of reference stars and photometric calibrations. The results are also listed in Table 1.

3.3. Skinakas Observations

About 5.5 hr after the GRB, the afterglow was also caught by the Roper/Photometrics CH360 CCD camera (SITe 1024×1024 chip), which was mounted in parallel with the OPTIMA-Burst instrument on the 1.3-m Skinakas Observatory telescope at Crete, Greece (Stefanescu et al. 2007). The field of view of the CCD camera is $\sim 8.5' \times 8.5'$. Again the data were reduced in the same way as the Xinglong data and included in Table 1.

3.4. Swift UVOT Observations

The *Swift* UVOT photometry in Table 1 was derived using data extracted from the official online UVOT GRB afterglow catalogue (Romig et al. 2009). The UVOT started observing the GRB since ~ 110 sec after the BAT trigger. A fading afterglow was detected in the *UVOT-white*, *V*, *B*, *U*, *UVW1*, and *UVM2* bands, but not in the bluest *UVW2* band. When needed we combined raw data of neighboring epochs, taking both the coincidence loss

corrected source count rate and background count rate, to make signal-to-noise ratio (S/N) larger than 3. But in the B , $UVW1$, and $UVM2$ bands we had to keep the data with $2.6 \lesssim S/N \lesssim 3$ which could mean a marginal detection.

The $UVOT$ observations lasted till very late time, ~ 10 days in the U band, ~ 3.4 days in the $UVOT$ -white band, and ~ 1.4 day in the rest. From the very late-time detections, which are not included in Table 1, we derived host-galaxy brightness of about 21.25 ± 0.15 , 21.75 ± 0.05 , and 21.5 ± 0.4 mag in the U , $UVOT$ -white, and $UVW1$ bands, respectively.

3.5. Multi-band Optical Light Curves

As shown in Figure 1, the flux of the optical afterglow decayed smoothly following a single power law in all bands and throughout the whole observation period, including the X-ray plateau phase. This is best demonstrated by the well-sampled R -band LC. The fitting power-law indices α of the flux evolution $f \propto t^\alpha$ are all similar, i.e., -1.05 ± 0.02 for R , -0.94 ± 0.11 for V , -0.98 ± 0.06 for B , -0.86 ± 0.07 for U , ~ -1 for $UVW1$, and -0.90 ± 0.18 for $UVM2$. The R -band LC was built using both the genuine R -band observations and the unfiltered TNT observations which have been approximately reduced to the R -band. But the Maidanak and Skinakas R -band data after 10,000 sec were not included in the fitting process due to the relatively large scatter among the data.

The late-time photometry must have been contaminated to some extent by the light of the host galaxy, which has been found by Levan et al. (2007) to be one of the brightest for GRBs. Those authors measured $R = 22.0 \pm 0.5$ mag, while using the host-galaxy spectrum published by them we derived $V \sim 22.4 \pm 0.5$ mag.

The optical LCs after subtracting the host galaxy contribution can also be well fitted by a single power law, with the slopes of each band slightly steeper but closer to one another, than before the subtraction. Specifically, we obtained $\alpha_R = -1.08 \pm 0.02$, $\alpha_V = -0.98 \pm 0.11$, $\alpha_U = -1.10 \pm 0.10$, and $\alpha_{UVW1} \sim -1.1$. The values are also similar to those of the X-ray LC before and after the plateau phase.

The optical afterglow did not evolve in synchronism with X-rays, being lack of any LC features that would correspond to the two breaks defining the beginning and end of the X-ray plateau. Similar behaviors were also observed in a few other bursts detected in the *Swift* era, e.g., GRB 050319 (Quimby et al. 2006) and GRB 070420 (Klotz et al. 2008). There have been many theoretical discussions (e.g., Fan & Piran 2006; Panaitescu et al. 2006) on that deviation to the standard afterglow model, but no satisfactory interpretation so far.

4. The X-ray Plateau, Fast Optical Decay and Energy Injection Model

It has become well known that the X-ray plateau phase can not be understood with the standard afterglow model (Fan & Piran 2006; Panaitescu et al. 2006). The standard model gives a shallow LC decay only if $\nu_c < \nu < \nu_m$, where ν_m is the minimum synchrotron frequency and ν_c the cooling frequency (see Zhang & Mészáros 2004). The model decay index $\alpha = -0.25$ may be similar to $\alpha_X^{\text{mid}} = -0.19 \pm 0.08$ of GRB 060912A, but the model photon index $\Gamma = -1.5$ is clearly inconsistent with the observed $\Gamma_X^{\text{mid}} = -2.08 \pm 0.11$.

During the X-ray plateau phase of the GRB, the X-ray frequency must be $\nu_X > \max\{\nu_m, \nu_c\}$, while the optical one ν_{opt} is probably between ν_m and ν_c , in the context of both the X-ray and optical afterglows coming from the same forward-shock synchrotron radiation process. The model spectral index $\beta \equiv \Gamma + 1$ as a function of the electron index p is $-p/2$ for $\nu > \max\{\nu_m, \nu_c\}$, $1/3$ for $\nu < \min\{\nu_m, \nu_c\}$, and in between either $(1-p)/2$ (slow cooling) or $-1/2$ (fast cooling). The expressions are the same between the standard model and its extension to include the energy injection scenario or that for the $1 < p < 2$ case (see Zhang & Mészáros 2004 and Zhang et al. 2006). Our analysis of the spectral energy distribution (SED) in the following section indicates that the intrinsic optical spectral index is probably > -0.7 . Therefore the optical photons must come from a model spectral segment different from that of the X-rays. On the other hand, ν_{opt} can not be $< \min\{\nu_m, \nu_c\}$ since it is highly unlikely that the extinction was so large as to make a positive intrinsic β_{opt} . Finally, to reconcile the spectral index $(1-p)/2$ between ν_m and ν_c with the observed $\beta_X^{\text{mid}} = -1.1$ would require an electron spectrum of $p \gtrsim 3$ which is too steep.

The X-ray plateau of the GRB may be explained using the energy injection model, which assumes an energy injection rate proportional to t^{-q} ($q < 1$) (Zhang et al. 2006). Since $\nu_X^{\text{mid}} > \max\{\nu_m, \nu_c\}$, we obtain $p \approx 2.2 \pm 0.2$ by equating $-p/2$ with $\beta_X^{\text{mid}} \approx -1.1 \pm 0.1$, which is most reasonable for an astronomical relativistic electron spectrum. The model predicts that $p = -2 + (8 - 4\alpha_X^{\text{mid}})/(q+2)$, and hence $q \approx 0.07 \pm 0.12$. Such a small q seems close to the case of energy injection due to pulsar spin-down (Dai & Lu 1998; Zhang & Mészáros 2001), and is consistent with the average value of -0.07 ± 0.35 found by Liang, Zhang & Zhang (2007) for their *Swift* sample.

The X-ray LC and spectrum after the plateau phase as the energy injection has ended also suggests an electron index of $\sim 2.1 - 2.2$. The observed $\alpha_X^{\text{late}} = -1.19 \pm 0.05$ and $\Gamma_X^{\text{late}} = -1.95 \pm 0.13$ satisfy the closure relationship $\alpha(\beta)$ only if $\nu > \max\{\nu_m, \nu_c\}$, in which case the standard model has $\alpha = (2 - 3p)/4$ and $\beta = -p/2$ (Zhang & Mészáros 2004).

However, the energy injection hypothesis is not applicable to the simultaneous fast optical LC decay observed throughout the X-ray plateau phase. Only for the slow-cooling

case of the wind scenario, the model LC between ν_m and ν_c can decay faster than $\nu > \max\{\nu_m, \nu_c\}$. But the model prediction, $\alpha_{\text{opt}} = \alpha_X - (2 - q)/4$, would compare with the observation, i.e., $\alpha_{\text{opt}} \sim -1$, only if $q \lesssim -1$, contradicting the above estimate of $q \approx 0.07 \pm 0.12$ as constrained by the observed β_X^{mid} and α_X^{mid} .

5. The Spectral Energy Distribution and Dust Extinction

We select $t = 700$ sec to build the optical-to-X-ray spectral energy distribution (SED), shown in Figure 2 as *filled squares*. Around the epoch, observational data can be found in the largest number of photometric bands. The host-subtracted magnitudes are listed in Table 2. The small flux change between the real data epoch and $t = 700$ sec has been corrected for, adopting the LC power-law indices as given in §3.5, as well as a small Galactic reddening of $E(B - V) = 0.05$. For the B and $UVM2$ bands of no host measurement, we assumed that the intrinsic afterglow flux should be ~ 0.05 mag fainter than the total, taking the host-subtracted results in the other bands as references. The optical magnitudes were converted into monochromatic fluxes using the conversion factors and effective frequencies taken from Poole et al. (2008) and Bessel, Castelli & Plez (1998). The X-ray flux is drawn at 1.73 keV in the figure, with *dotted lines* indicating spectrum uncertainties.

For comparison, we built also the SED at $t = 7,000$ sec (Figure 2; *open squares*). Only the optical data in the R , V and U bands and the X-ray data were used in order to avoid large uncertainties caused by host galaxy contamination and data interpolation.

By power-law fitting, we obtained an optical-to-X-ray spectral index of $\beta_{\text{OX}} = 0.7 \pm 0.1$ for both epochs. First, the GRB clearly does not belong to the “optically” dark bursts ($\beta_{\text{OX}} < 0.5$; Jakobsson et al. 2004; Zheng, Deng & Wang 2009). Secondly, at $t = 700$ sec the optical fluxes in the $UVW1$ and $UVM2$ bands fall much below the optical-to-X-ray fitting power law, suggesting either strong dust extinction in the host galaxy or hydrogen Lyman line absorption. We further suggest that the intrinsic spectrum of the optical afterglow during the X-ray plateau phase is probably shallower than $\nu^{-0.7}$ and hence the optical band lies between ν_m and ν_c at the epoch. If we instead assume an intrinsic optical spectral index equivalent to the X-ray one, the extinction-corrected β_{OX} will still be considerably larger than $\beta_X^{\text{mid}} = -1.08$ for any of the MW ($\beta_{\text{OX}} \approx -0.86$), LMC ($\beta_{\text{OX}} \approx -0.78$), and SMC ($\beta_{\text{OX}} \approx -0.75$) extinction laws. A special artificially fine-tuned flat extinction law would be required to make the optical-to-X-ray SED as steep as the X-ray spectrum itself, which is beyond the scope of this paper (but see Chen, Li & Wei 2006).

The flux loss caused by H Lyman absorption was ~ 0.11 mag in the $UVM2$ band

and ~ 0.07 mag in the *UVW1* band. Most absorption probably occurred in the host-galaxy damped-Ly α system that gave rise to the large X-ray $N_{\text{H}}^{\text{host}}$ of $\sim 4.2 \times 10^{21} \text{ cm}^{-2}$, as estimated by us assuming a Voigt line profile taking into account thermal-Doppler broadening and natural broadening. The intergalactic hydrogen contributed only ~ 0.02 mag in *UVM2* and ~ 0.01 mag in *UVW1* at $z = 0.937$, according to the formulae of Madau et al. (1996). In our calculations, when doing flux integration, a power law spectrum of $f_{\nu} \propto \nu^{-0.6}$ was assumed and the *UVOT* filter response curves of Poole et al. (2008) were adopted.

In the 700-sec SED, the *B*-band flux falls well below both the *V* band flux and the *U* band one, which seems to suggest the interesting possibility of a 2175-Å dust extinction feature from the host galaxy. One could argue that the *V*-band flux may be overestimated since it looks larger than the *R*-band one. But we note that it is also above the simple interpolation from the *R*-band to the *U*-band, so evidence of extra extinction in the *B*-band is unambiguous. Such a feature is characteristic of the dust extinction law of the MW, displaying a full width of $\sim 700 \text{ \AA}$ (Cardelli et al. 1989). It does not exist in the extinction law of the SMC, while being rather modest in the LMC one (Pei 1992). At $z = 0.937$, it is almost entirely located in the observer-frame *UVOT B*-band (Poole et al. 2008).

We tested the three dust-extinction laws on the 700-sec optical SED, with the results shown in the *inset* of Figure 2. Note that the *UVW1* and *UVM2* bands have been corrected for the H Lyman absorption, after which the optical SED (*filled squares*) can be fitted with a power law of index $\sim -1.7 \pm 0.4$. As discussed above, the afterglow model predicts an intrinsic spectral index β_{opt} , i.e., after correction for dust extinction, of either -0.5 (fast cooling) or $(1 - p)/2$ (slow cooling), i.e., $\sim -0.5 - -0.7$ assuming $p \sim 2.0 - 2.4$. Thereafter, we took -0.6 ± 0.1 as the reference value of β_{opt} and reproduced it with the extinction-corrected optical SED by adjusting the reddening value $E(B - V)$. The results are $E(B - V) = 0.25 \pm 0.02$ for the MW extinction law, ~ 0.15 for the LMC case, and ~ 0.1 the SMC.

As shown in the figure (*filled circles*), the MW-like extinction well corrects the observed flux deficiency in the *B* band. This is just as expected and in stark contrast to the cases of LMC (*open circles*) and SMC (*open squares*). Note that here we did not use the common minimum- χ^2 approach to constrain the extinction. A minimum power-law fitting χ^2 were obtained for a much smaller $E(B - V)$, resulting in a corrected optical SED too steep to comply with the general afterglow model and a reasonable extension to the X-ray spectrum.

A MW-like dust extinction law may also be supported by the fact that the host galaxy is one of the brightest among long GRBs (Levan et al. 2007; see also Savaglio, Glazebrook & Le Borgne 2009). Brighter galaxies tend to have an evolved stellar population and higher metallicity. After correcting the published host galaxy spectrum for redshift, we synthesized its absolute *B*-band magnitude and obtained $M_B < -21.5$ even before extinction correc-

tions. So the galaxy must have metallicity near or even higher than the solar value, or $Z \equiv 12 + \log(\text{O}/\text{H}) > 8.9 \pm 0.6$ according to the Kobulnicky & Kewley (2004) M_B - Z relationship for $z \in [0.8, 1.0]$. It is significantly higher than most GRB host galaxies ($\sim 7.4 - 8.7$; Savaglio, Glazebrook & Le Borgne 2009), LMC (~ 8.3), and SMC (~ 8.0). On the other hand, the dust-to-gas ratio, $A_V/N_{\text{H}}^{\text{host}}$, is smaller than the empirical values of the MW, LMC, and SMC, just as the other GRB host galaxies (Schady et al. 2007).

Although the GRB is not optically dark, it may belong to the “dim” category of optical afterglows as defined by Liang & Zhang (2006) and Nardini et al. (2006). Using the two fitting LCs shown in Figure 1, we derived the host-subtracted observer-frame R -band magnitude at $(1+z)12\text{hr}$ of $\sim 23.1 \pm 0.4$, corrected for the Galactic extinction. This was then converted to a rest-frame 12-hr R -band luminosity assuming the observed optical SED of $f_\nu \propto \nu^{-1.7 \pm 0.4}$ (see Figure 2). Finally, after the host-galaxy extinction of $A_R \sim 0.5$ (MW-like law) was corrected for, we obtained an intrinsic afterglow luminosity of $L(\nu_R, 12\text{hr}) \sim 1.9 \pm 0.8 \times 10^{29}$ erg. The latest dim afterglow sample, compiled by Nardini, Ghisellini & Ghirlanda (2008), has a mean value of $\langle \log L(\nu_R, 12\text{hr}) \rangle = 29.3$.

6. Discussion

With GRB 060912A, we have added another case to a few puzzling GRBs that show achromatic X-ray LC breaks at the beginning and end of a plateau phase which are not present in the optical band. Unlike the original sample compiled by Panaitescu et al. (2006) and those supplemented by other authors (e.g., Melandri et al. 2008), in current case the optical temporal index is quite similar to the contemporaneous X-ray one before and after the X-ray plateau. Although the optical and X-ray characteristics during the X-ray plateau are difficult to explain self-consistently just as the others, the standard afterglow model can actually apply to the rest stages of this GRB. The optical afterglow showed little if any evolution in its temporal index and optical colors, so it likely arose from the same synchrotron spectral segment throughout, or specifically $\nu_m < \nu_{\text{opt}} < \nu_c$ of the ISM and slow-cooling case, while the post-plateau X-ray afterglow must have $\nu_X > \nu_c$ as demonstrated by its slightly steeper LC slope and a significant spectral deviation from the optical-to-X-ray SED. There could be a cooling break around the beginning of the X-ray plateau, but we do not have the early X-ray spectrum to either argue for or against this. In overall our data analysis seems to support a hypothesis that the optical and X-ray afterglows are of the same origin except for the X-ray plateau which is dominated by an extra component (Panaitescu 2008a). Other explanations like a reverse-shock afterglow (Uhm & Beloborodov 2007; Genet, Daigne & Mochkovitch 2007) and the “late prompt” emission (Ghisellini et al. 2009) are not favored for this GRB.

An evolution of microphysical parameters (e.g., Fan & Piran 2006; Ioka et al. 2006) is not excluded providing that it is strictly associated with the energy injection process. A quantitative comparison between our data and the theory of Panaitescu (2008a) may be possible but is beyond the scope of this paper.

We have shown evidence of a 2175-Å extinction feature in the optical SED of the GRB 060912A afterglow. Such a feature has only been observed in a very small number of GRBs, which may also include GRB 970508 (Stratta et al. 2004), GRB 991216 (Kann, Klose & Zeh 2006; Vreeswijk et al. 2006), GRB 050802 (Schady et al. 2007), GRB 070802 (Krühler et al. 2008; Elíasdóttir et al. 2009), GRB 080607 (Prochaska et al. 2009), and possibly even the high-redshift GRB 050904 (Liang & Li 2009). Only the identification in GRB 070802 can be regarded as robust since the feature was detected not only through multi-color photometry but also clearly in a spectrum. In the other cases, the feature was merely revealed as a dip in the corresponding passband in the observed optical SED. Although the afterglow spectrum of GRB 991216 also displayed a similar feature, it centers at a somewhat “wrong” position, about 2360 Å, (Vreeswijk et al. 2006). This UV absorption bump is the most prominent feature of the MW extinction law and is now widely hypothesized to be caused by a mixture of large polycyclic aromatic hydrocarbon molecules or clusters, whose strong C-C bond $\pi \rightarrow \pi^*$ transitions peak at ~ 2175 Å, and small carbon-rich grains (Drain 2003 and references therein). Both species are thought to be fragile under the illumination of strong UV and X-ray radiation (e.g., Voit 1992; Fruchter, Krolik & Rhoads 2001), so the reported absorption likely took place a few parsecs away from the GRB location (Perna & Lazzati 2002; but see Liang & Li 2009). It was suggested that the UV bump requires a relatively evolved stellar population, which means less dust/molecule destruction by UV photons or interstellar shocks, in order to explain its absence in the SMC and most starburst galaxies (Gordon, Calzetti & Witt 1997; Noll et al. 2007). So it is not surprising that the majority of GRB afterglow SEDs are best fitted using a SMC extinction law (e.g., Kann, Klose & Zeh 2006; Schady et al. 2007; Starling et al. 2007) since they are typically hosted in faint dwarf star-forming galaxies. On the other hand, among the few cases with a reported UV bump, GRB 050802, GRB 060912A, and GRB 070802 all have a host galaxy unusually bright (possibly $M_B \lesssim -21 - -22$; see Fynbo et al. 2005, Elíasdóttir et al. 2009, Levan et al. 2007, and this paper) for a GRB, while the faint host galaxy of GRB 970508 has an early-type morphology (Savaglio, Glazebrook & Le Borgne 2009). Finally we note that when the paper is written a statistical study made by Schady et al. (2009) is published which also presents the UVOT SED of GRB 060912A, but those authors seem prudent not to claim the observed *B*-band flux depression a detection of the 2175-Å feature.

We thank E. Liang for the electronic files of the X-ray data. This work was supported

by the National Basic Research Program of China (Grant No. 2009CB824800) and by the NSFC (Grant No. 10673014).

REFERENCES

- Amati L., et al. 2008, MNRAS, 391, 577.
- Bessel, M. J., Castelli, F. & Plez, B. 1998, A&A, 333, 231.
- Cardelli, J. A., Clayton, G. C., & Mathis, J. S. 1989, ApJ, 345, 245.
- Chen, S. L., Li, A., & Wei, D. M. 2006, ApJ, 647, L13.
- Dai, Z.-G., & Lu, T. 1998, A&A, 333, L87
- Deng, J., Zheng, W., Zhai, M. Qiu, Y., Wei J., & Hu, J. 2006, IL Nuovo Cimento B, 121, 1469.
- Deng, J., Zheng, W., L. Xin, Zhai, M., Qiu, Y., Wei J., & Hu, J. 2008, in AIP Conf. Proc. 1065, 2008 Nanjing GRB Conf., eds. Y. Huang, Z. Dai, & B. Zhang (?: AIP), 107.
- Drain, B. T. 2003, ARA&A, 41, 241.
- Elíasdóttir, Á, et al. 2009, ApJ, 697, 1725.
- Fan, Y., & Piran, T. 2006, MNRAS, 369, 197.
- Fruchter, A., Krolik, J. H., & Rhoads, J. E. 2001, ApJ, 563, 597.
- Fynbo J. U., et al. 2005, GCN Circ. 3756.
- Gehrels, N., Ramirez-ruiz, E., & Fox, D. B. 2009, ARA&A, 47, 567.
- Genet, F., Daigne, F., & Mochkovitch, R. 2007, MNRAS, 381, 732.
- Ghisellini, G., Nardini, M., Ghirlanda, G., & Celotti, A. 2009, MNRAS, 393, 253,
- Golenetskii, S., et al. 2006, GCN 5570.
- Gordon, K. D., Calzetti, D., & Witt, A. N. 1997, ApJ, 487, 625.
- Granot, J. 2008, preprint (arXiv:0811.1657).
- Hurkett, et al. 2006, GCN 5558.

- Hurkett, C. P., Page, K. L., & Rol, E. 2006, GCN 5562.
- Ioka, K., Toma, K., Yamazaki, R., & Nakamura, T. 2006, *Å0*, 458, 7.
- Jakobsson, P., Hjorth, J., Fynbo, J. P. U., Watson, D., Pedersen, K., Björnsson, G., & Gorosabel, J. 2004, *ApJ*, 617, L21.
- Kann, D. A., Klose, S., & Zeh, A. 2006, *ApJ*, 641, 993.
- Kobulnicky, H. A., & Kewley, L. J. 2004, *ApJ*, 617, 240.
- Klotz, A., et al. 2008, *A&A*, 483, 847.
- Krühler, T., et al. 2008, *ApJ*, 685, 376.
- Levan, A. J., et al. 2007, *MNRAS*, 378, 1439.
- Li, A., Liang, S. L., Kann, D. A., Wei, D. M., Klose, S., & Wang, Y. J. 2008, *ApJ*, 685, 1046.
- Liang, E.-W., & Zhang, B. 2006, *ApJ*, 638, L67.
- Liang, E.-W., Zhang, B.-B., & Zhang, B. 2007, *ApJ*, 670, 565.
- Liang, S. L., & Li, A. 2009, *ApJ*,
- Madau, P., Ferguson, H. C., Dickinson, M. E., Giavalisco, M., Steidel, C. C., & Fruchter, A. 1996, *MNRAS*, 283, 1388.
- Melandri, A., et al. 2008, *ApJ*, 686, 1209.
- Nardini, M., Ghisellini, G., Ghirlanda, G., Tavecchio, F., Firmani, C., & Lazzati, D. 2006, *A&A*, 451, 821.
- Nardini, M., Ghisellini, G., & Ghirlanda, G. 2008, *MNRAS*, 386, L87.
- Noll, S., Pierini, D., Pannella, M., & Savaglio, S. 2007, *A&A*, 472, 455.
- Oates, S. R., et al. 2009, *MNRAS*, 395, 490.
- Panaitescu, A., Meszaros, P., Burrow, D., Nousek, J., Gehrels, N., O'Brien, P., & Willingale, R. 2006, *MNRAS*, 369, 2059.
- Panaitescu, A. 2008, *MNRAS*, 383, 1143.

- Panaiteescu, A. 2008, in AIP Conf. Proc. 1111, Probing stellar populations out to the distant universe, eds. (?: AIP), 362
- Parsons, A., et al. 2006, GCN 5561.
- Pei, Y. C. 1992, ApJ, 395, 130.
- Perna, R., & Lazzati, D. 2002, ApJ, 580, 261.
- Poole, T. S., et al. 2008, MNRAS, 627, 645.
- Prochaska, J. X., et al. 2009, ApJ, 691, L27.
- Quimby, R. M., et al. 2006, ApJ, 640, 402.
- Roming, P. W. A., et al. 2009, ApJ, 690, 163.
- Sakamoto, T., et al. 2008, ApJS, 175, 179.
- Sakamoto, T., et al. 2009, ApJ, 693, 911.
- Savaglio, S., Glazebrook, K., & Le Borgne, D. 2009, ApJ, 691, 182.
- Schady, B., et al. 2007, MNRAS, 377, 273.
- Schady, B., et al. 2009, MNRAS, in press.
- Stefanescu, A., et al. 2007, Astronomische Nachrichten, 328, 620.
- Starling, R. L. C., et al. 2007, ApJ, 661, 787.
- Stratta, G., Fiore, F., Antonelli, L. A., Piro, L., & De Pasquale, M. 2004, ApJ, 608, 846.
- Uhm, Z., & Beloborodov, A. 2007, ApJ, 665, L93.
- Voit, G. M. 1992, MNRAS, 258, 841.
- Vreeswijk, P. M., et al. 2006, A&A, 447, 145.
- Zheng, W., et al. 2008, Chinese J. Astron. Astrophys., 8, 693.
- Zheng, W., Deng, J., & Wang, J. 2009, RAA, 9, 1103.
- Zhang, B., & Mészáros, P. 2001, ApJ, 552, L35.
- Zhang, B., & Mészáros, P. 2004, Int. J. Mod. Phys. A, 19, 2385.

Zhang, B., et al. 2006, ApJ, 642, 354.

Zhang, B. 2007, ChJAA, 7, 1.

Zhang, B. 2007, Adv. Space Res., 40, 1186.

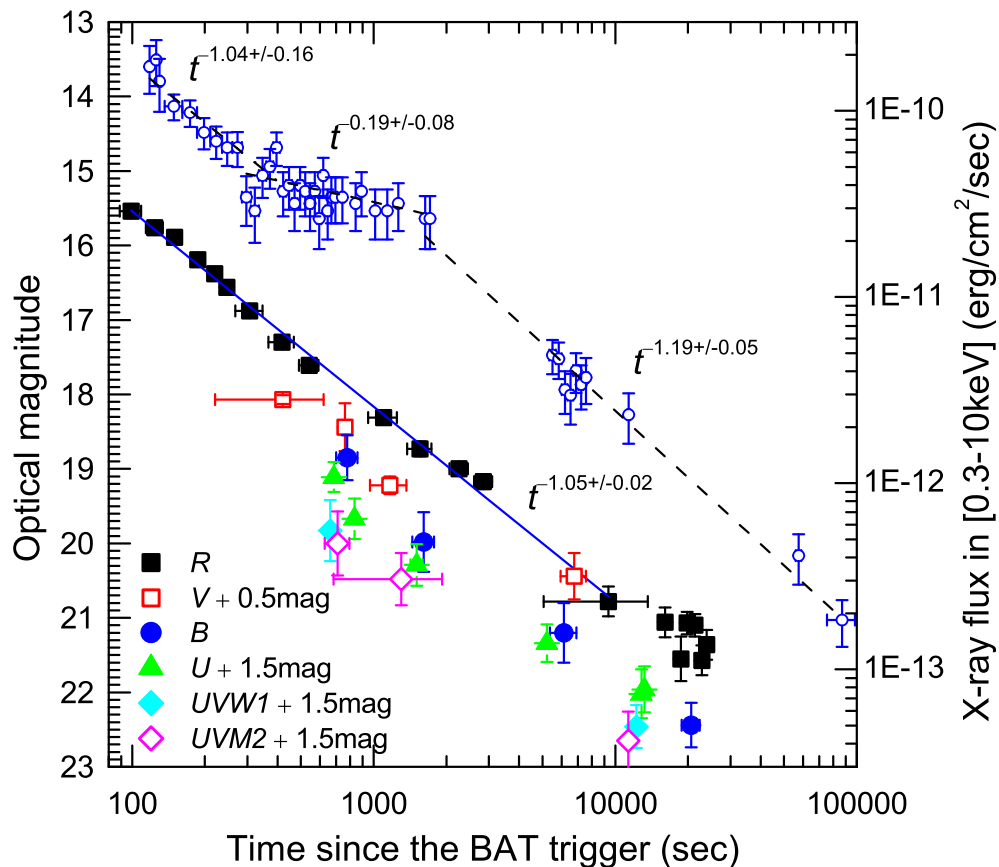


Fig. 1.— Observed optical light curves of GRB 060912A afterglow plotted in magnitude in the R (filled squares), V (open squares), B (filled circles), U (triangles), $UVW1$ (filled diamonds), and $UVM2$ (open diamonds) bands, compared with the flux evolution in the $[0.3 - 10 \text{ keV}]$ X-ray band (open circles). Also shown are power-law fits (dashed lines) to the three X-ray LC segments, and that to the observed R -band flux before the subtraction of the host galaxy flux (solid line).

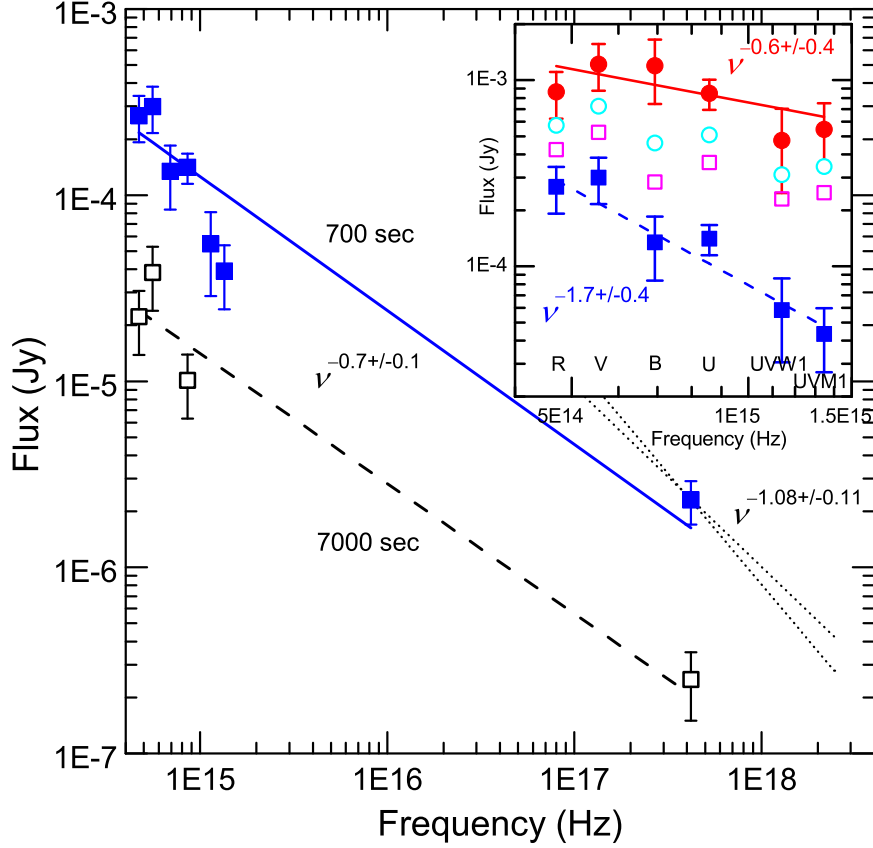


Fig. 2.— *Main panel:* Optical-to-X-ray SEDs of GRB 060912A afterglow at 700 sec (*filled squares*) and 7,000 sec (*open squares*) after the BAT trigger, with no correction of optical fluxes for H Lyman absorption and host dust extinction. Also shown are power-law fits to the SEDs (*solid* and *dashed* lines) and the fitting power-law X-ray spectra at 700 sec (*dotted lines*). *Inset:* Optical SEDs of GRB 060912A afterglow at 700 sec, either uncorrected for host dust extinction (*filled squares*) or corrected assuming the MW (*filled circles*), LMC (*open circles*) and SMC (*open squares*) extinction law, respectively, while H Lyman absorption and Galactic dust extinction has also been corrected. Also shown are power-law fits to the MW case (*solid line*) and host extinction-uncorrected case (*dashed line*).

Table 1. Optical photometry of GRB 060912A afterglow

| mean time (sec) ^a | span (sec) ^b | R_C | <i>white</i> ^c | V | B | U | $UVW1$ | $UVM2$ | $UVOT$ - <i>white</i> | telescope ^d |
|------------------------------|-------------------------|------------|---------------------------|------------|-------------------------|------------|------------|------------|-----------------------|------------------------|
| 9.90E1 | 20 | ... | 15.54±0.08 | ... | ... | ... | ... | ... | ... | TNT |
| 1.24E2 | 20 | ... | 15.76±0.08 | ... | ... | ... | ... | ... | ... | TNT |
| 1.50E2 | 20 | ... | 15.89±0.08 | ... | ... | ... | ... | ... | ... | TNT |
| 1.65E2 | 100 | ... | ... | ... | ... | ... | ... | ... | 16.66±0.03 | UVOT ^e |
| 1.87E2 | 20 | ... | 16.19±0.08 | ... | ... | ... | ... | ... | ... | TNT |
| 2.20E2 | 20 | ... | 16.38±0.08 | ... | ... | ... | ... | ... | ... | TNT |
| 2.47E2 | 20 | ... | 16.56±0.08 | ... | ... | ... | ... | ... | ... | TNT |
| 3.07E2 | 80 | ... | 16.88±0.08 | ... | ... | ... | ... | ... | ... | TNT |
| 4.17E2 | 100 | ... | 17.30±0.08 | ... | ... | ... | ... | ... | ... | TNT |
| 4.20E2 | 400 | ... | ... | 17.57±0.06 | ... | ... | ... | ... | ... | UVOT |
| 5.41E2 | 100 | ... | 17.61±0.08 | ... | ... | ... | ... | ... | ... | TNT |
| 6.60E2 | 20 | ... | ... | ... | ... | ... | 18.33±0.41 | ... | ... | UVOT |
| 6.84E2 | 20 | ... | ... | ... | ... | 17.61±0.20 | ... | ... | ... | UVOT |
| 7.10E2 | 170 | ... | ... | ... | ... | ... | ... | 18.50±0.43 | ... | UVOT |
| 7.17E2 | 10 | ... | ... | ... | ... | ... | ... | ... | 18.70±0.22 | UVOT |
| 7.60E2 | 20 | ... | ... | 17.94±0.32 | ... | ... | ... | ... | ... | UVOT |
| 7.77E2 | 160 | ... | ... | ... | 18.85±0.30 | ... | ... | ... | ... | UVOT |
| 8.32E2 | 20 | ... | ... | ... | ... | 18.17±0.27 | ... | ... | ... | UVOT |
| 9.10E2 | 100 | ... | ... | ... | ... | ... | ... | ... | 18.62±0.07 | UVOT |
| 1.10E3 | 300 | 18.31±0.07 | ... | ... | ... | ... | ... | ... | ... | TNT |
| 1.16E3 | 400 | ... | ... | 18.72±0.12 | ... | ... | ... | ... | ... | UVOT |
| 1.30E3 | 1240 | ... | ... | ... | ... | ... | ... | 18.98±0.35 | ... | UVOT |
| 1.47E3 | 10 | ... | ... | ... | ... | ... | ... | ... | 18.70±0.21 | UVOT |
| 1.51E3 | 180 | ... | ... | ... | ... | 18.79±0.28 | ... | ... | ... | UVOT |
| 1.56E3 | 360 | 18.73±0.10 | ... | ... | ... | ... | ... | ... | ... | TNT |
| 1.61E3 | 340 | ... | ... | ... | 19.98±0.40 | ... | ... | ... | ... | UVOT |
| 1.79E3 | 10 | ... | ... | ... | ... | ... | ... | ... | 19.24±0.33 | UVOT |
| 2.26E3 | 400 | ... | 19.00±0.08 | ... | ... | ... | ... | ... | ... | TNT |
| 2.85E3 | 480 | 19.17±0.10 | ... | ... | ... | ... | ... | ... | ... | TNT |
| 3.64E3 | 600 | ... | ... | ... | 20.07 (UL) ^f | ... | ... | ... | ... | TNT |
| 3.80E3 | 300 | ... | ... | 19.40 (UL) | ... | ... | ... | ... | ... | TNT |
| 4.53E3 | 1260 | ... | ... | ... | 20.60 (UL) | ... | ... | ... | ... | 60cm |
| 5.22E3 | 200 | ... | ... | ... | ... | 19.84±0.25 | ... | ... | ... | UVOT |
| 5.63E3 | 200 | ... | ... | ... | ... | ... | ... | ... | 20.61±0.19 | UVOT |
| 6.14E3 | 1530 | ... | ... | ... | 21.20±0.40 | ... | ... | ... | ... | UVOT |

Table 1—Continued

| mean time (sec) ^a | span (sec) ^b | R_C | <i>white</i> ^c | V | B | U | $UVW1$ | $UVM2$ | $UVOT$ - <i>white</i> | telescope ^d |
|------------------------------|-------------------------|------------|---------------------------|------------|------------|------------|------------|------------|-----------------------|------------------------|
| 6.75E3 | 1630 | ... | ... | 19.94±0.31 | ... | ... | ... | ... | ... | UVOT |
| 7.06E3 | 200 | ... | ... | ... | ... | ... | ... | ... | 20.86±0.23 | UVOT |
| 9.35E3 | 8600 | 20.78±0.20 | ... | ... | ... | ... | ... | ... | ... | TNT |
| 1.13E4 | 900 | ... | ... | ... | ... | ... | ... | 21.15±0.39 | ... | UVOT |
| 1.22E4 | 900 | ... | ... | ... | ... | ... | 20.96±0.29 | ... | ... | UVOT |
| 1.28E4 | 300 | ... | ... | ... | ... | 20.52±0.33 | ... | ... | ... | UVOT |
| 1.32E4 | 440 | ... | ... | ... | ... | 20.46±0.31 | ... | ... | ... | UVOT |
| 1.61E4 | 600 | 21.06±0.20 | ... | ... | ... | ... | ... | ... | ... | 1.5m |
| 1.87E4 | 960 | 21.55±0.30 | ... | ... | ... | ... | ... | ... | ... | 1.5m |
| 1.99E4 | 600 | 21.07±0.15 | ... | ... | ... | ... | ... | ... | ... | 1.3m |
| 2.06E4 | 3600 | ... | ... | ... | 22.44±0.30 | ... | ... | ... | ... | 1.5m |
| 2.14E4 | 1800 | 21.10±0.15 | ... | ... | ... | ... | ... | ... | ... | 1.3m |
| 2.28E4 | 2160 | 21.57±0.20 | ... | ... | ... | ... | ... | ... | ... | 1.5m |
| 2.39E4 | 1800 | 21.36±0.20 | ... | ... | ... | ... | ... | ... | ... | 1.3m |

^aMiddle time for a single exposure, or exposure-time-weighted mean time for multiple exposures.

^bTime span from the beginning of first exposure to the end of last exposure.

^c R -band equivalent; TNT unfiltered photometry calibrated using R -band reference stars.

^dThe telescopes are the 80-cm TNT and 60-cm of Xinglong Obs., 1.3-m of Skinakas Obs., 1.5-m of Maidanak Obs., and UVOT of *Swift*.

^eThe UVOT photometry is derived using data extracted from http://swift.gsfc.nasa.gov/docs/swift/results/uvot_grb/cat/.

^fUL means an upper limit only.

Table 2. Host galaxy-subtracted magnitudes ^a at different epochs

| epoch (sec) | R_C | V | B | U | $UVW1$ | $UVM2$ |
|-------------|-----------------|-----------------|-----------------|-----------------|-----------------|-----------------|
| 700 | 17.78 ± 0.3 | 17.87 ± 0.3 | 18.79 ± 0.4 | 17.68 ± 0.2 | 18.46 ± 0.5 | 18.55 ± 0.4 |
| 7,000 | 20.48 ± 0.4 | 20.10 ± 0.4 | ... | 20.54 ± 0.4 | ... | ... |

^aThe small Galactic reddening of $E(B - V) = 0.05$ has not been corrected for.